

## Optimizing the growth of 1.3 $\mu\text{m}$ InAs/GaAs quantum dots

P. B. Joyce, T. J. Krzyzewski, G. R. Bell, and T. S. Jones

*Centre for Electronic Materials and Devices, Department of Chemistry, Imperial College, London, SW7 2AY, United Kingdom*

E. C. Le Ru and R. Murray

*Centre for Electronic Materials and Devices, Department of Physics, Imperial College, London SW 2BZ, United Kingdom*

(Received 21 May 2001; published 20 November 2001)

Scanning probe microscopy has been used to show that InAs/GaAs quantum dots (QD's) can be grown (at very low growth rates) using continuous InAs depositions of up to five monolayers (ML) without QD coalescence. These growth conditions result in relatively large coherent QD's which exhibit strong room temperature photoluminescence (PL) at a wavelength of 1.3  $\mu\text{m}$  when capped with GaAs. The average QD volume prior to capping increases monotonically with InAs coverage up to 5 ML, but the PL emission wavelength saturates around 1.3  $\mu\text{m}$  after  $\sim 3$  ML. This is due to the presence of much larger, irregular and plastically relaxed three-dimensional islands which act as sinks for additional deposited material and do not participate in optical emission.

DOI: 10.1103/PhysRevB.64.235317

PACS number(s): 68.35.Bs, 68.37.Ef, 78.66.Fd

### I. INTRODUCTION

The growth of self-assembled InAs/GaAs quantum dot (QD) structures has been studied extensively in recent years, with a particular technological emphasis on optoelectronic devices such as lasers and light-emitting diodes. There is strong interest in the production of QD structures which emit light at 1.3  $\mu\text{m}$  (0.95 eV), a longer wavelength than typically achieved for this material system.<sup>1,2</sup> Various methods to extend the emission wavelength to 1.3  $\mu\text{m}$  and to improve the sharpness of the emission peak have been explored.<sup>3-9</sup> Growth interrupts appear to cause red-shifts or blueshifts depending on the amount of InAs deposited and the point of interruption during capping, but this approach does lead to a reduction in the emission linewidth.<sup>3-5</sup> The use of a "strain reduction layer" (SRL), composed of  $\text{In}_x\text{Ga}_{1-x}\text{As}$  rather than GaAs, to either cap or surround the QD's has been widely employed to achieve 1.3  $\mu\text{m}$  emission with narrow linewidths.<sup>6-10</sup> We have demonstrated a particularly simple method for producing 1.3  $\mu\text{m}$  emission by using very low InAs deposition rates ( $< 0.02 \text{ ML s}^{-1}$ ) during growth by conventional molecular beam epitaxy (MBE). Scanning tunneling microscopy (STM) and atomic force microscopy (AFM) studies of the uncapped QD's showed a reduction in QD density and an increase in the average QD size.<sup>11,12</sup> The observed red-shift in emission was attributed to the low growth rate QD's having a very high InAs content. By contrast, conventional growth rates ( $> 0.1 \text{ ML s}^{-1}$ ) result in significant alloying<sup>13</sup> and lower In content QD's, which emit at shorter wavelength.

For conventional MBE growth conditions (growth rate  $> 0.1 \text{ ML s}^{-1}$ , temperature  $\sim 500^\circ\text{C}$ ), the island density saturates rapidly after the two-dimensional (2D)  $\rightarrow$  3D growth mode transition and coalescence of the QD's typically occurs when around 3.0 ML of InAs has been deposited.<sup>14,15</sup> The reduction in QD number density at low growth rates provides the opportunity to deposit larger amounts of InAs before island coalescence. In this paper, we present a quantitative study of "high InAs coverage" QD's, using up to 5.0 ML

InAs deposits. STM and AFM are used to characterize the uncapped QD's whilst photoluminescence (PL) spectroscopy is used to investigate their optical properties when capped with GaAs. It is shown that for ultralow growth rates ( $< 0.02 \text{ ML s}^{-1}$ ), room temperature emission saturates at  $\sim 1.3 \mu\text{m}$ , and this value cannot be exceeded either by increased InAs deposition or by further reductions in the InAs deposition rate.

### II. EXPERIMENTAL DETAILS

The samples used for STM, AFM, and PL analysis were all grown in a combined MBE-STM system (DCA Instruments/Omicron GmbH), also equipped with reflection high energy electron diffraction (RHEED). Growth was monitored by RHEED, while RHEED intensity oscillations were used to calibrate all material fluxes. Ultralow InAs growth rates, for which direct RHEED oscillation data were unobtainable, were calibrated by extrapolation from data obtained at growth rates above  $0.08 \text{ ML s}^{-1}$ . Epiready GaAs(001) substrates ( $n^+$ , silicon doped) were mounted on molybdenum sample plates and transferred directly into the MBE chamber via a fast entry load lock chamber. After initial thermal cleaning at  $300^\circ\text{C}$ , the native oxide layer was removed under an  $\text{As}_2$  flux at  $620^\circ\text{C}$  ( $\text{As}_2$  beam pressure  $2.6 \times 10^{-6} \text{ mbar}$ ). A 600 nm GaAs buffer layer was grown at  $590^\circ\text{C}$  and a rate of 500 nm per hour, before the substrate temperature was reduced to  $510^\circ\text{C}$  for the deposition of a further 30 nm of GaAs. InAs was then deposited at one of several fixed growth rates (0.003 to  $0.13 \text{ ML s}^{-1}$ ), without growth interruption or periodic supply of As and In species, to coverages between 1.8 and 5.0 ML. This paper focuses mainly on low ( $\sim 0.015 \text{ ML s}^{-1}$ ) to ultralow ( $\sim 0.003 \text{ ML s}^{-1}$ ) growth rates, for which InAs deposition times as long as 25 min were used. After InAs deposition, samples for STM or AFM analysis were immediately quenched from the MBE chamber into the ultrahigh vacuum STM chamber. This process takes only a few seconds and eliminates any effect of post-growth annealing. Constant current STM im-

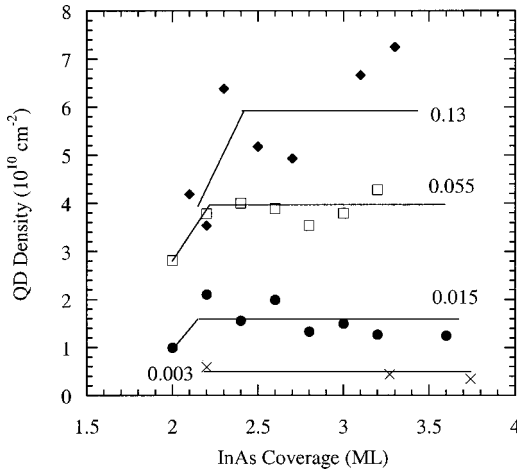


FIG. 1. The number density of InAs/GaAs QD's measured by STM and AFM as a function of InAs coverage for four different deposition rates (0.003, 0.015, 0.055, and 0.13  $\text{ML s}^{-1}$ ). The lines are guides to the eye.

ages were obtained using a tunneling current of 0.1–0.3 nA and a sample bias of  $-3.5$  V. These measurements were supported by *ex situ* AFM studies.

The growth of samples for PL measurements differed only after the deposition of InAs was complete. Instead of quenching to the STM chamber, they were capped immediately with 40 nm of GaAs at  $510^\circ\text{C}$  before the substrate temperature was returned to  $590^\circ\text{C}$  for a final GaAs capping thickness of 100 nm. *Ex situ* PL measurements were carried out at 10 and 300 K. HeNe or  $\text{Ar}^+$  lasers were used to create electron-hole pairs and the luminescence was dispersed with a SPEX 1404 monochromator. Light was detected with a cooled Ge photodiode and lock-in amplifier.

### III. RESULTS

The QD number density measured by STM and AFM for uncapped samples is shown in Fig. 1 as a function of growth rate and coverage. The number density at coverages above 2.2 ML drops by an order of magnitude from  $(6 \pm 1) \times 10^{10} \text{ cm}^{-2}$  to  $(5 \pm 1) \times 10^9 \text{ cm}^{-2}$  as the growth rate is lowered from 0.13 to 0.003  $\text{ML s}^{-1}$ . The QD number density is essentially independent of coverage for values greater than  $\sim 2.2$  ML, suggesting that the nucleation of new QD's is complete within 0.4 ML of the 2D $\rightarrow$ 3D growth mode transition which at this temperature occurs at  $\sim 1.8$  ML.<sup>13</sup> STM and AFM images show clearly that even for high coverages ( $\sim 0.5$  ML) no coalescence of the QD's occurs at the lowest growth rates because of the low number density. This behavior contrasts with that at conventional growth rates where the much higher number density leads to coalescence after  $\sim 3.0$  ML.<sup>14</sup> In addition, high resolution STM images indicate that the underlying wetting layer (WL) has a characteristic, disordered  $(1 \times 3)$  reconstruction, consistent with the presence of an  $\text{In}_x\text{Ga}_{1-x}\text{As}$  alloy.<sup>16,17</sup> The appearance of the WL is similar to that found at conventional growth rates<sup>13,16</sup> and shows no changes as the InAs coverage is increased.

*In situ* STM was also used to make detailed measure-

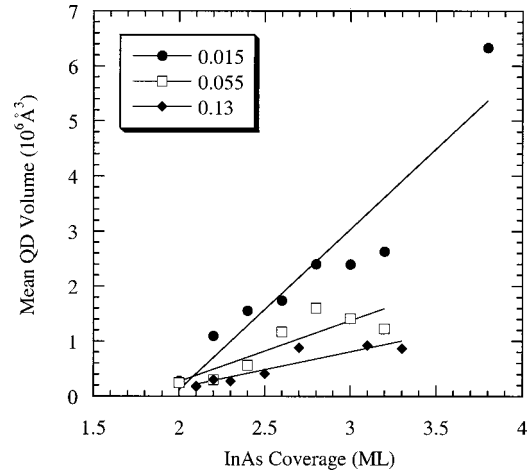


FIG. 2. The mean QD volume determined by STM as a function of InAs coverage for three different deposition rates (0.015, 0.055, and 0.13  $\text{ML s}^{-1}$ ). The solid lines are linear fits.

ments of the characteristics of the uncapped QD's for coverages between 2.0 and 3.8 ML. Base diameters, heights and volumes were measured for many individual QD's at each growth rate and coverage. The QD volumes were obtained using image processing software which directly integrates the STM topograph over each QD, avoiding any assumptions about QD shape. The effects on the average QD volume of increasing InAs coverage are shown in Fig. 2. Tip convolution is a potential problem with all volume and shape estimations by scanning probe microscopy, but this was minimized in the STM measurements by rejecting images where strong tip convolution was apparent as well as by *in situ* tip treatment.<sup>18</sup> As a result, only three reliable data points were available at the lowest growth rate (0.003  $\text{ML s}^{-1}$ ) due to a combination of increased tip convolution and poorer statistics from the low number density. Figure 2 clearly indicates an increase in mean QD volume which is approximately linear with the coverage beyond the 2D $\rightarrow$ 3D transition. Between 2.0 and 3.8 ML the average QD volume changes from  $2.8 \times 10^5 \text{ \AA}^3$  ( $\sim 1.1 \times 10^4$  atoms) to  $6.3 \times 10^6 \text{ \AA}^3$  ( $\sim 2.6 \times 10^5$  atoms) for a growth rate of 0.015  $\text{ML s}^{-1}$ . A similar trend is observed even at 0.003  $\text{ML s}^{-1}$ , with the mean QD volume being around  $\sim 1.0 \times 10^7 \text{ \AA}^3$  ( $\sim 4.1 \times 10^6$  atoms) for coverages  $> 3.5$  ML.

We have previously established that a considerable degree of In-Ga intermixing (“alloying”) occurs during the formation of QD's at conventional temperatures and growth rates.<sup>11,13</sup> It was possible to infer the presence of GaAs in QD's grown at 0.13  $\text{ML s}^{-1}$  and  $500^\circ\text{C}$  by calculating the total QD volume and comparing this to the total volume of InAs deposited.<sup>13</sup> Since the former was found to be much greater than the latter, an increase of the QD size by WL and substrate erosion was implied. This effect is reduced by growing at lower temperatures<sup>13</sup> or at lower rates.<sup>11</sup> The total QD volume for growth at  $510^\circ\text{C}$  and 0.015  $\text{ML s}^{-1}$  as a function of coverage is shown in Fig. 3, where the solid line represents ideal Stranski-Krastanov (SK) growth (i.e., no alloying) with a critical thickness of 1.8 ML. The data collapse on to this line, implying that there is no excess Ga in the

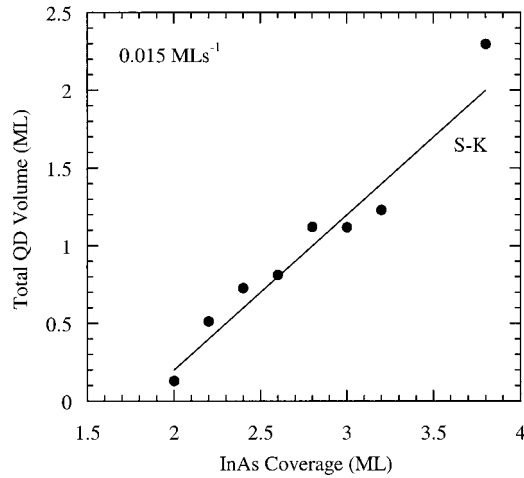


FIG. 3. The total QD volume per unit area (in ML equivalents) as a function of InAs coverage at a growth rate of  $0.015 \text{ ML s}^{-1}$ . The solid line is that expected for ideal Stranski-Krastanov growth (no alloying) with a critical thickness of 1.8 ML.

QD's and that they are pure InAs.<sup>11</sup> Ideal SK growth was also found for all lower growth rates studied.

PL spectra were obtained at 10 K from GaAs capped QD samples. The peak emission energy is shown in Fig. 4 as a function of InAs coverage at three different growth rates. Increasing the InAs coverage at  $0.015 \text{ ML s}^{-1}$  leads to a redshift from 1.13 eV ( $1.11 \mu\text{m}$ ) at 2.2 ML to 1.06 eV ( $1.17 \mu\text{m}$ ) at 4.5 ML. At lower growth rates (0.010 and  $0.006 \text{ ML s}^{-1}$  are shown) the emission energy is essentially independent of InAs coverage, and saturates around 1.04 eV (corresponding to  $1.3 \mu\text{m}$  at room temperature). Increasing the InAs coverage has no significant effect on the linewidth and all three growth rates exhibit relatively narrow emission lines with a full width at half maximum (FWHM) of  $32 \pm 5 \text{ meV}$ . Increasing the coverage beyond 3.5 ML at  $0.015 \text{ ML s}^{-1}$  reduces the PL intensity, particularly at room tem-

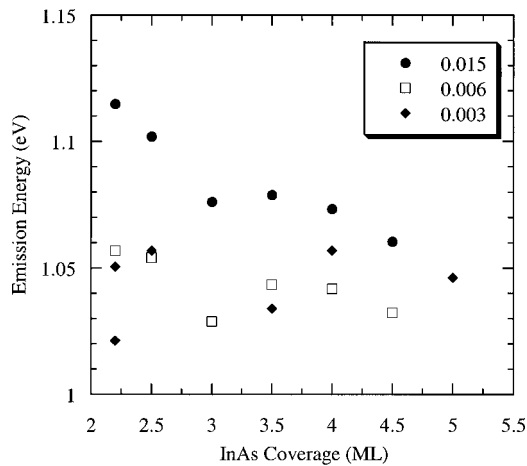


FIG. 4. The low temperature PL emission energy from capped InAs/GaAs QD samples grown at three different rates ( $0.015$ ,  $0.006$ , and  $0.003 \text{ ML s}^{-1}$ ) as a function of InAs coverage. Only the highest growth rate shows a clear variation in the emission energy as a function of coverage.

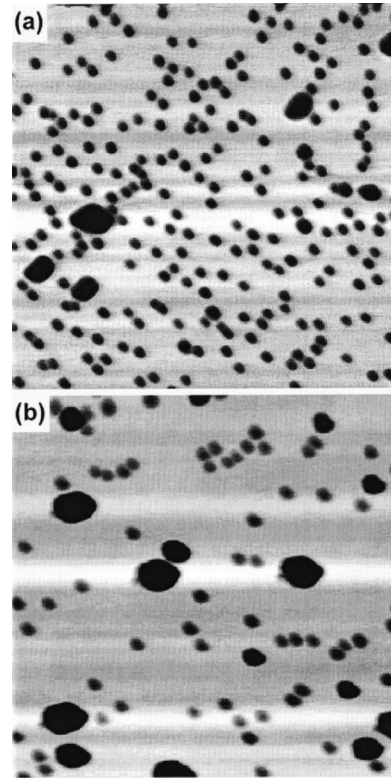


FIG. 5. Two AFM images,  $1.4 \mu\text{m} \times 1.4 \mu\text{m}$ , of 3.6 ML InAs deposited on GaAs at growth rates of (a)  $0.015 \text{ ML s}^{-1}$  and (b)  $0.003 \text{ ML s}^{-1}$ .

perature. Similar reductions in PL efficiency are also observed at lower growth rates ( $0.006$  and  $0.003 \text{ ML s}^{-1}$ ) and are apparent at smaller InAs coverages.

Figure 5 shows two AFM topographs of 3.6 ML InAs grown at rates of (a)  $0.015 \text{ ML s}^{-1}$  and (b)  $0.003 \text{ ML s}^{-1}$ , obtained with the same AFM tip. The images show a bimodal QD size distribution. There is a large number of “regular” QD's and a small fraction of much larger islands, with a more irregular shape. The mean height of regular QD's is  $100 \pm 5 \text{ \AA}$  for all growth rates  $< 0.015 \text{ ML s}^{-1}$ . In the two cases shown in Fig. 5 the mean heights are 97 and  $100 \text{ \AA}$ , respectively. The height fluctuation of the two QD arrays is also approximately the same (counting only regular QD's) at 7%. Apart from the differences in the QD number density, the most obvious distinction between the two AFM images is the relative density and size of the large irregular islands. For the QD arrays grown at  $0.015 \text{ ML s}^{-1}$  the average height of the irregular islands is  $200 \text{ \AA}$  and the number density ( $N_i$ ) is  $3 \times 10^8 \text{ cm}^{-2}$ , implying a relative density (irregular/regular) of 3%. At the lower growth rate of  $0.003 \text{ ML s}^{-1}$  the average height of the irregular islands is  $420 \text{ \AA}$  and the relative density is 13% ( $N_i = 4 \times 10^8 \text{ cm}^{-2}$ ). The total volume of material contained in the large irregular islands is therefore much higher at lower growth rates. Our preliminary TEM studies reveal the presence of dislocations within the large irregular islands, but not in the regular QD's.

The QD volume distribution obtained by STM for a growth rate of  $0.015 \text{ ML s}^{-1}$  is shown in Fig. 6. For each coverage the mean, the 50th percentiles and the 95th percen-

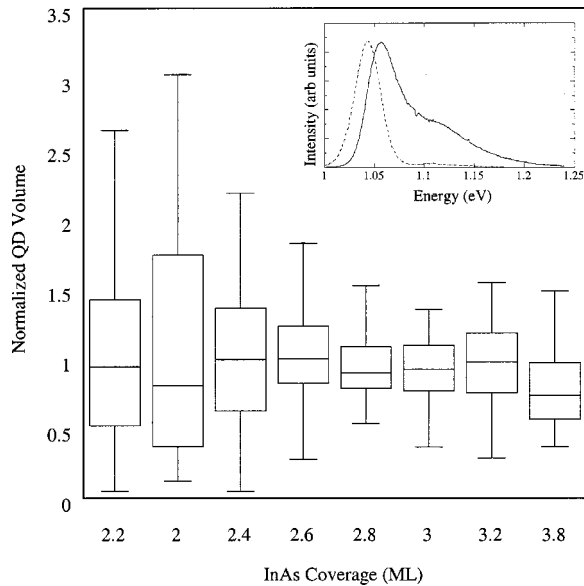


FIG. 6. A representation of the QD volume distribution (see text) for various coverages between 2.0 and 3.8 ML and a growth rate of  $0.015 \text{ ML s}^{-1}$ . Volumes are normalized to the average volume at each coverage. The inset shows PL spectra obtained from two QD samples grown at  $0.006 \text{ ML s}^{-1}$ ; the InAs coverages are 2.2 ML (solid line) and 3.5 ML (dashed line).

tiles of the distribution are represented by a central horizontal line, a box and vertical lines, respectively. As the coverage is increased from 2.0 to 2.6 ML there is a marked narrowing of the size distribution, while there is insignificant change in the width for higher coverages. The inset of Fig. 6 shows low temperature PL spectra obtained from two QD samples with an InAs coverage of 2.2 ML (solid line) and 3.5 ML (dashed line) grown at  $0.006 \text{ ML s}^{-1}$ . The low coverage sample exhibits a highly skewed shape with a high energy shoulder. Reducing the laser intensity produces no change in the shape of the distribution suggesting that the shoulder is not due to excited states of a single family of QD sizes, but rather a result of ground state emission from the smaller QD's. In comparison the higher coverage sample shows no evidence of a shoulder.

#### IV. DISCUSSION

Several factors affect the emission wavelength and line-width of encapsulated QD's including the mean QD size and size fluctuation, the composition of the QD's and the surrounding material, and the strain state of the QD's. All of these can be influenced by both the QD growth conditions (principally growth rate, temperature, and InAs coverage) and by the capping conditions. In the present study, the substrate temperature and GaAs capping rate are fixed and only InAs coverage and growth rate are altered. Even without a detailed knowledge of the composition, size and shape of the capped QD's in the present study, it is possible to rationalise all of the observed changes in emission characteristics on the basis of the initial changes in the structural characteristics of the uncapped QD arrays.

At an InAs growth rate of  $0.015 \text{ ML s}^{-1}$  the emission

energy is reduced as the InAs coverage increases (Fig. 4). This can be related simply to the increasing size of the QD's with coverage (Fig. 2) and is consistent with simple finite well calculations, which predict that larger QD's have a smaller confinement energy and hence emit at lower energies. The composition of these QD's prior to GaAs capping is close to 100% InAs for all coverages, as shown by the SK-like behavior of the total volume (Fig. 3 and Ref. 11). It is known that the composition and shape of the QD's can be altered significantly by the capping process<sup>19–21</sup> and we might expect that smaller QD's are more strongly affected by In-Ga intermixing during capping due to their higher surface area to volume ratio. If this is the case, then larger uncapped QD's would maintain a higher In fraction and hence emit at lower energies. This effect would be cumulative with that of the initial QD size in determining the emission energy, and both are consistent with the observed behavior. In the absence of detailed compositional information on capped QD structures grown under these conditions, we cannot separate the effects of composition change and initial size. However, the observed behavior of the emission energy at the highest growth rate is easily explained by a combination of these mechanisms.

By contrast, for the lower growth rates ( $0.006$  and  $0.003 \text{ ML s}^{-1}$ ) there is no correlation between the InAs coverage and the emission energy, which remains at  $1.04 \pm 0.02 \text{ eV}$  for all coverage studied (Fig. 4). This is despite the fact that the mean QD volume increases linearly with coverage (Fig. 2) and following the arguments given in the previous paragraph, one would expect a continued redshift with higher coverage. To rationalize the observed behavior, it is necessary to take into account the large irregular 3D islands that are particularly apparent in the *ex situ* AFM images (Fig. 5). As discussed in Sec. III, the size and density of these large 3D islands increases as the growth rate is lowered. Hence, at ultralow growth rates, although SK growth is preserved, a much larger fraction of the additional deposited InAs is incorporated into these irregular islands. The regular QD's show no significant increase in size at high coverages or ultralow growth rates, with a maximum height of around  $100 \text{ \AA}$ . If the optical emission is due only to these regular, coherent QD's then the independence of emission energy with coverage is not surprising since these regular QD's do not evolve significantly with increased coverage.

The growth rates of elastically strained versus plastically relaxed 3D islands have been discussed experimentally in the SiGe system<sup>22</sup> and theoretically.<sup>23</sup> The latter analysis is quite general and suggests that the growth rate of partially relaxed islands containing misfit dislocations is higher than that of an elastically relaxed dislocation-free coherent island of the same size.<sup>22</sup> There is an energy barrier to dislocation formation and also a minimum island size for this to become favorable. These findings are consistent with the present results in which incoherent, irregular islands grow rapidly with increasing coverage while the regular QD's do not grow as much. We note that bimodal/skewed QD size distributions<sup>24</sup> and large,<sup>25</sup> irregular 3D island have also been observed in the InAs-GaAs system. These irregular islands may well have an important role in both suppressing the nucleation of

new QD's at higher coverages (leading to rapid saturation of the number density, Fig. 1) and in allowing the development of narrow size distributions among elastically relaxed "regular" QD's. The rapid saturation in the mean height of the regular QD's even over a large coverage range (at least 3 to 5 ML) provides strong evidence for a maximum preferred QD size ( $>2 \times 10^5$  atoms) at which attachment of adatoms to irregular islands becomes more favorable. The exact mechanism of the formation of these large irregular islands is unknown and will be the subject of further investigation.

The presence of large islands containing dislocations also influences the PL emission intensity obtained from the various samples. For lower growth rates and the highest coverages at  $0.015 \text{ ML s}^{-1}$  the PL emission intensity is weaker, particularly at room temperature. This can be attributed to nonradiative recombination in the vicinity of dislocations, the probability of which increases as the ratio of plastically relaxed islands to regular QD's increases. At higher temperatures the probability of carrier escape is much higher and carriers can transfer to the plastically relaxed islands via the wetting layer. It is possible to avoid the formation of a large fraction of irregular giant islands by keeping the growth rate  $\geq 0.01 \text{ ML s}^{-1}$ . This growth rate and a coverage of around 3.5 ML (total InAs deposition time  $\sim 6$  min) is sufficient to push the low temperature emission energy to  $1.2 \mu\text{m}$ , and hence achieve  $\sim 1.3 \mu\text{m}$  at room temperature while maintaining good PL efficiency. The insensitivity of the PL linewidth to the InAs coverage for the low growth rates also fits with the idea that only the regular QD's participate in optical emission. There is little change in the height fluctuation of the regular QD's (7–9%) for coverages  $>2.5$  ML and growth rates  $<0.015 \text{ ML s}^{-1}$ , and hence the observed linewidth remains around 32 meV for all these samples.

Finally, we turn to the regime of relatively low coverage (2–2.5 ML). For the ultralow growth rates the density of irregular islands is  $<10\%$  of the QD density at these coverages, while the mean QD size is still increasing linearly with coverage. However, the emission energy does not appear to deviate significantly from the saturation value at higher coverages ( $>2.5$  ML). Since at lower growth rates there is a lower number density of QD's from the onset of nucleation (Fig. 1), the QD's are expected to reach their maximum size much quicker than at higher growth rates and hence changes in the emission energy are more difficult to detect for coverages in the range 2–3 ML (Fig. 4). At  $0.015 \text{ ML s}^{-1}$ , we observe a high energy shoulder in the PL spectrum only for coverages  $<2.5$  ML (Fig. 6, inset). This can be explained by

the presence of many developing QD's which are significantly smaller than the maximum size, i.e., are still accepting a large fraction of the incoming material. Such QD's appear as the low-volume tails of the distribution functions represented in Fig. 6. As both the progressive narrowing of the distributions occurs ( $>2.5$  ML, Fig. 6) and the mean QD size increases (Fig. 2), this tail of developing QD's disappears along with the high energy PL peak shoulder.

## V. CONCLUSIONS

We have studied the effects of InAs coverage on the properties of InAs/GaAs QD's produced at very low growth rates. QD's can be grown using continuous InAs depositions of up to five monolayers (ML) at very low growth rates without island coalescence. For growth rates below  $\sim 0.01 \text{ ML s}^{-1}$  and InAs coverages above  $\sim 2.5$  ML, the QD's show strong optical emission at  $1.04 \pm 0.02 \text{ eV}$  with narrow linewidths of  $32 \pm 5 \text{ meV}$  at 10 K. These values do not change despite significant differences in the mean QD sizes at different growth rates and coverages. The reason for this behavior is the presence of two distinct types of 3D island, namely regular elastically relaxed QD's with narrow height distributions (100 Å, fluctuation  $\sim 7\%$ ) and large, irregular, plastically relaxed 3D islands. The latter increase in density and size at high coverages and ultralow growth rates, acting as sinks for additional deposited material, while the regular QD's hardly evolve with coverage. This provides strong evidence for a maximum preferred QD size over a wide range of coverages (3–5 ML) at this temperature. The regular QD's are solely responsible for the optical response while the irregular giant islands act as nonradiative recombination centers, reducing PL efficiency. A growth rate of  $0.01 \text{ ML s}^{-1}$  and a coverage  $\sim 3.5$  ML (6 min of InAs growth) gives optimum performance of the QD's, which emit at  $1.3 \mu\text{m}$  at room temperature without impaired efficiency and with narrow linewidth (32 meV). The density of the QD's is optimised at  $1 \times 10^{10} \text{ cm}^{-2}$ .

## ACKNOWLEDGMENTS

This work was supported by the Engineering and Physical Sciences Research Council (EPSRC), U.K. under Grant No. GR1N14040. P.B.J. and T.J.K. both acknowledge the EPSRC for support. G.R.B. is grateful to the Ramsay Memorial Trust for financial support, sponsored in part by VG Semicon Ltd. We are grateful to Jim Neave for many useful discussions and Diana Zhi for performing preliminary TEM studies.

<sup>1</sup>M. Grassi Alessi, M. Capizzi, A. S. Bhatti, A. Frove, F. Martelli, P. Frigeri, A. Bosacchi, and S. Franchi, *Phys. Rev. B* **59**, 7620 (1999).

<sup>2</sup>L. Chu, M. Arzberger, G. Bohm, and G. Abstreiter, *J. Appl. Phys.* **85**, 2355 (1999).

<sup>3</sup>Z. D. Lu, J. Z. Xu, B. Z. Zheng, Z. Y. Lu, and W. K. Ge, *Solid State Commun.* **109**, 649 (1999).

<sup>4</sup>J. M. Gerard, J. B. Genin, J. Lefevre, J. M. Moison, N. Lebouche,

and F. Barthe, *J. Cryst. Growth* **150**, 351 (1995).

<sup>5</sup>H. Wang, Z. Niu, H. Zhu, Z. Wang, D. Jiang, and S. Feng, *Physica B* **279**, 217 (2000).

<sup>6</sup>V. M. Ustinov, A. E. Zhukov, N. A. Maleev, S. S. Mirkhrin, A. F. Tsatsul'nikov, M. V. Maximov, B. V. Volovik, D. A. Bedarev, P. S. Kop'ev, Z. I. Alferov, L. E. Vorob'ev, D. A. Firsov, A. A. Suvorova, P. Werner, N. N. Ledenstov, and D. Bimberg, *Microelectron. J.* **31**, 1 (2000).

- <sup>7</sup>V. M. Ustinov, N. A. Maleev, A. E. Zhukov, A. R. Kovsh, A. Yu. Egorov, A. V. Lunev, B. V. Volovik, I. L. Krestnikov, Yu. H. Musikhin, N. A. Bert, P. S. Kop'ev, and Zh. I. Alferov, *Appl. Phys. Lett.* **74**, 2815 (1999).
- <sup>8</sup>H. Liu, X. Wang, J. Wu, B. Xu, Q. Wei, W. Jiang, D. Ding, X. Ye, F. Lin, J. Zhang, J. Liang, and Z. Wang, *J. Appl. Phys.* **88**, 3392 (2000).
- <sup>9</sup>N.-T. Yeh, T.-E. Nee, J.-I. Chyi, T. M. Hsu, and C. C. Huang, *Appl. Phys. Lett.* **76**, 1567 (2000).
- <sup>10</sup>K. Nishi, H. Saito, S. Sugou, and J. Lee, *Appl. Phys. Lett.* **74**, 1111 (1999).
- <sup>11</sup>P. B. Joyce, T. J. Krzyzewski, G. R. Bell, T. S. Jones, S. Malik, D. Childs, and R. Murray, *Phys. Rev. B* **62**, 10 891 (2000).
- <sup>12</sup>R. Murray, D. Childs, S. Malik, P. Sivers, C. Roberts, J-M Hartmann, P. Stavrinou, *Jpn. J. Appl. Phys.* **38**, 528 (1999).
- <sup>13</sup>P. B. Joyce, T. J. Krzyzewski, G. R. Bell, B. A. Joyce, and T. S. Jones, *Phys. Rev. B* **58**, R15 981 (1998).
- <sup>14</sup>J. M. Moison, F. Houzay, F. Barthe, L. Leprince, E. Andre, and O. Vates, *Appl. Phys. Lett.* **64**, 196 (1994).
- <sup>15</sup>D. Leonard, K. Pond, and P. M. Petroff, *Phys. Rev. B* **50**, 11 687 (1994).
- <sup>16</sup>J. G. Belk, C. F. McConville, J. Sudijono, T. S. Jones, and B. A. Joyce, *Surf. Sci.* **387**, 283 (1997).
- <sup>17</sup>M. Sauvage-Simkin, Y. Garreau, R. Pinchaux, M. B. Veron, J. P. Landesman, and J. Nagle, *Phys. Rev. Lett.* **75**, 3485 (1995).
- <sup>18</sup>Tip convolution is generally obvious in STM due to the irregular nature of the etched tungsten tips employed, but is rather less obvious in the AFM studies.
- <sup>19</sup>D. Zhi, H. Davock, R. Murray, C. Roberts, T. S. Jones, D. W. Pashley, P. J. Goodhew, and B. A. Joyce, *J. Appl. Phys.* **89**, 2079 (2001).
- <sup>20</sup>J. M. Garcia, G. Medeiros-Ribeiro, K. Schmidt, T. Ngo, J. L. Feng, A. Lorke, J. Kotthaus, and P. M. Petroff, *Appl. Phys. Lett.* **71**, 2014 (1997).
- <sup>21</sup>P. B. Joyce, T. J. Krzyzewski, G. R. Bell, and T. S. Jones, *Surf. Sci.* **492**, 345 (2001).
- <sup>22</sup>M. Krishnamurthy, J. S. Drucker, and J. A. Venables, *J. Appl. Phys.* **69**, 6461 (1991).
- <sup>23</sup>J. Drucker, *Phys. Rev. B* **48**, 18 203 (1993).
- <sup>24</sup>V. P. Evtikhiev, V. E. Tokranov, A. K. Kryganovskii, A. M. Boiko, R. A. Suris, and A. N. Titkov, *J. Cryst. Growth* **201/202**, 1154 (1999).
- <sup>25</sup>I. Kamiya, I. Tanaka, and H. Sakaki, *J. Cryst. Growth* **201/202**, 1146 (1999).